

# Concepts and Combustion Characteristics of an Ultra-micro and a Micro Combustor

YUASA Saburo, OSHIMI Kana and UEHARA Mamiko<sup>1</sup>

<sup>1</sup>Tokyo Metropolitan Institute of Technology,  
Asahigaoka 6-6, Hino-city, Tokyo 191-0065, JAPAN  
Phone: +81-42-585-8657, FAX: +81-42-583-5119, E-mail: syuasa@cc.tmit.ac.jp

## ABSTRACT

We have proposed two types of hydrogen-fueled micro combustors: one is for an Ultra Micro Gas Turbine (UMGT) generating a 16-W output and the other is for a Micro Gas Turbine (MGT) generating a 3-kW output.

For the ultra-micro combustor of the UMGT, we clarified the most important issues, such as quenching distance, heat losses, shortened diffusion characteristic time and flow laminarization. This clarification led to a unique burning method, which is called the flat-flame burning method. A prototype of a flat-flame ultra-micro combustor with a volume of 0.067 cm<sup>3</sup> was made and tested. It was found that the flame stability region of the flat-flame, which is governed by the heat losses in the combustor, satisfied the optimum operation region of the UMGT. The combustion efficiency achieved was more than 99.2 %. The excellence of the flat-flame burning method in the ultra-micro combustor for the UMGT was confirmed.

For the MGT with a 3-kW output, an annular-type hydrogen-fueled combustor with an air flow rate of 50 g/s was designed, and a sector-model test combustor of the annular combustor was made to determine its combustion characteristics. By using swirlers with a strong swirl intensity and four-hole fuel injectors, outstanding performance was attained for flame stability, space heating rate, temperature distribution and combustion efficiency.

## INTRODUCTION

Recently, micro gas turbines have been a growing interest as a distributed electrical power generating system. One of the practical systems is an Ultra Micro Gas Turbine (UMGT) using hydrogen, which was proposed by an MIT group with the following specifications: pressure ratio 4, air mass flow rate  $\dot{m}_a = 0.15$  g/s, combustor exit temperature 1600 K, fuel mass flow rate  $\dot{m}_f = 7$  g/hr, combustion chamber volume 0.07 cm<sup>3</sup>, rotor speed  $2.4 \times 10^6$  rpm and power output 16 W (Epstein, et al., 1997). This system will potentially be applied to mobile devices and micro-robots, as well as micro-thrusters for airplanes. The other practical system is a Micro Gas Turbine (MGT), which generates power in the range of a few kilowatts. The MGT will potentially have applications in home-size cogeneration systems and human-type robots. However,

the actualization of the ultra-micro and micro gas turbines as a whole system requires many technical breakthroughs for the individual components constituting gas turbines. In this paper, we focused on an ultra-micro and a micro combustor, because they have not yet adequately satisfied the performances required for UMGT and MGT.

For the ultra-micro combustor, the objectives of this paper are to clarify the issues related to downsizing the combustors, and then, based on the issues, to propose a new burning concept for UMGT, to build a prototype ultra-micro combustor using hydrogen fuel, and to examine its performance experimentally. For the micro combustor, the objectives are to design a compact combustor that matches the compressor-turbine system using a turbocharger for passenger cars, to make a test combustor, and finally to examine its combustion characteristics.

## ULTRA-MICRO COMBUSTOR

### PROBLEMS OF MINIATURIZATION AND BURNING CONCEPT

#### Significant problems

In order to downsize a combustor, the characteristic problems, which are mostly ignored in conventional gas turbine combustors must be overcome. The particular factors contributing to these problems are as follows;

- Relative increase of quenching distance
- Higher heat losses due to the high surface-to-volume ratio
- Shortened diffusion characteristic time
- Flow laminarization

The first three factors induce weak flame stability and combustion efficiency. The diffusion characteristic time is represented as  $L^2/D$  [ $L$ : length,  $D$ : diffusion coefficient]. When downsizing a flame, the shortened diffusion characteristic time has a crucial effect on the rapid uniformity of density distributions; an ultra-micro flame with the scale of an ordinary flame zone may dilute its fuel concentration, expand its flame zone, and decrease its temperature. Therefore, premixed combustion instead of diffusion combustion should be selected in micro combustors.

In general, flow laminarization prevents high space heating rates ( $SHR$ ) due to the low transport coefficients related to mass and heat transfer in combustors. In ultra-micro combustors, turbulent

combustion, which is employed in most conventional gas turbines in order to increase *SHR*, is not possible. Consequently, the realization of high *SHR* in a laminar flow is one of the prerequisites for UMG. T.

**Flat-flame burning method**

What a burning method is the most suitable for ultra-micro combustors? The Reynolds number for the ultra-micro combustor proposed by the MIT group was 100 ~ 200, which is 3 to 4 orders of magnitude lower than those for conventional combustors. This suggests that the flows in ultra-micro combustors would be laminar. For UMG. T, MEMS (Micro ElectroMechanical Systems) technology does not allow the use of the multi-stage, axis-low, three-dimensional turbo compressor and turbine currently used in high-performance gas turbines. MEMS technology is limited to a two-dimensional centrifugal turbo design. To accommodate this design, the shape of ultra-micro combustors must be a flat disk. One of the burning methods that forms a laminar flame in a disk-shaped combustor is a flat-flame burner, which has a porous flame holder introduced into the incoming premixture and stabilizes a flat-flame on the surface of the holder, thereby balancing the incoming flow velocity and the burning velocity of the premixture with heat conduction losses to the flame holder (Fristrom and Wstenberg, 1965). Therefore, a flat-flame is obtained when the burning velocity without heat losses is higher than the incoming flow velocity.

For the MIT UMG. T combustor, the incoming flow velocity was calculated to be about 0.6 m/s at the maximum cross section of the combustor. Moreover, the burning velocity of the hydrogen-air premixture at  $\phi = 0.4$ , which is required to achieve the combustor exit temperature of 1600 K, was obtained to be about 1.2 m/s experimentally. Consequently, for ultra-micro combustors, a laminar flat-flame may be stabilized on the porous plate placed at the maximum cross section of the combustor. If the height of the flat-flame micro combustor is equal to the flame zone thickness, *SHR* would be significantly high, thus satisfying the requirement level of UMG. T.

**ULTRA-MICRO COMBUSTOR AND EXPERIMENTAL PROCEDURE**

**Prototype ultra-micro combustor**

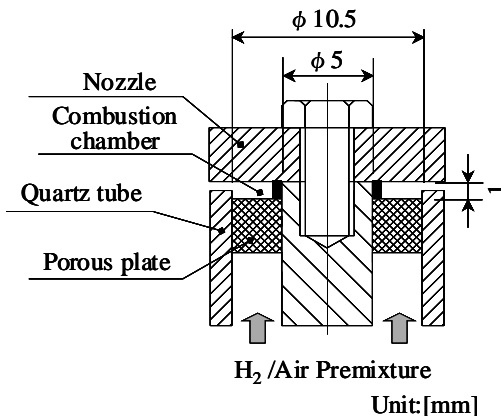


**Fig.1 Schematic of Flat-Flame ultra-micro combustor**

A schematic of the flat-flame ultra-micro combustor used in this study is shown in Fig. 1. The basic dimensions of the combustor were chosen from the UMG. T specifications proposed by the MIT group in 1997 (Epstein, et al., 1997). Each experiment was performed under atmospheric pressure and room temperature. The air mass flow rates  $\dot{m}_a$  were varied from 0.004 g/s to 0.094 g/s in order to make  $\dot{m}_a$  0.15 g/s at the pressure ratio of 4.

The combustor consists of a center shaft, a porous plate made of brass as an injector, an outer quartz tube, and a nozzle made of BN (boron nitride). The combustion chamber was an annular region with an inner and outer diameter of 5 mm and 10.5 mm, respectively. The height of the combustion chamber was 1 mm, and the volume is 0.067 cm<sup>3</sup>, which was almost equal to the final goal volume of the first MIT model. After combustion, the burned gas exits radially outward to the atmosphere through the slit between the nozzle and the quartz tube. Details of the apparatus and the procedure are described elsewhere (Yuasa and Oshimi, 2002).

**Measurement**

In this paper, the flame appearances, flame stability limits, temperature distributions, and combustion efficiency were measured. Ignition was achieved with a pilot flame from outside of the chamber. The temperature distributions were measured using a sheathed K thermocouple, 0.25 mm in diameter. The combustion efficiencies were calculated from the unburned hydrogen concentrations measured by inserting a quartz micro probe at the exit slit and using a hotwire-type semi-conductor hydrogen analyzer.

**EXPERIMENTAL RESULTS AND DISCUSSION**

**Flame appearance**

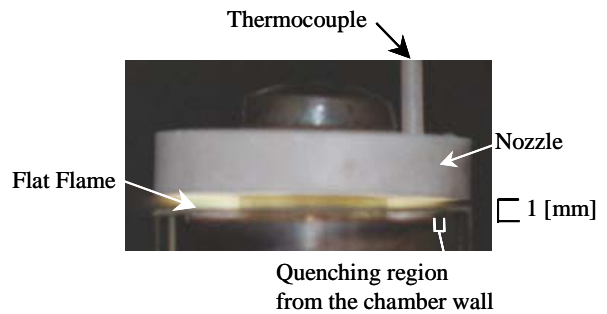


**Fig.2(a) Flat-flame at  $\dot{m}_a = 0.037$  g/s and  $\phi = 0.4$  (Hydrogen/Air)**

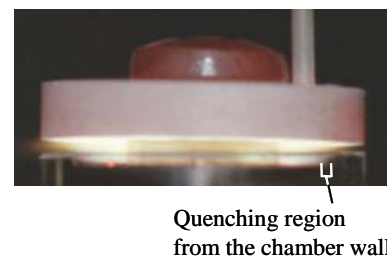


**Fig.2(b) Flat-flame at  $\dot{m}_a = 0.037$  g/s and  $\phi = 0.5$  (Hydrogen/Air)**

Figure 2(a) shows a typical flat-flame appearance formed in the ultra-micro combustor. [ $\dot{m}_a = 0.037$  g/s, the equivalence ratio of a hydrogen-air premixture;  $\phi = 0.4$ ]. This flame was very stable, occupied the whole volume of the combustion chamber, and burned well within this small space. Also, its appearance was similar to the premixed flames in the stagnation regions. Although a quenching region existed near the side wall of the chamber, this flat-flame satisfied the flat-flame burning method requirement, in that the flame zone was equal to the combustion chamber volume itself, so that it achieved extremely high *SHR*. Figure 2(b) shows a flat-flame at  $\dot{m}_a = 0.037$  g/s,  $\phi = 0.5$ . Compared with Fig. 2(a), although this flame did not show any change in appearance, an increase of heat loss to the nozzle due to a higher heat generation rate was inferred, since the screw on the nozzle turned red with heat.

**Flame stability limits**

The flame stability limits of this combustor are presented in Fig. 3, and they satisfied the design operation region of UMG combustors (assuming a 16-W power output). For lower limit, the minimum occurred at a  $\dot{m}_a$  around 0.037 g/s, then rose sharply as  $\dot{m}_a$  decreased, and then slightly increased as  $\dot{m}_a$  increased as well. The measurement, however, was performed under  $\dot{m}_a = 0.094$  g/s due to the limitation of the air and hydrogen mass flow meters.

Heat losses are considered to have a critical effect on the flame stability lower limit. In general, heat loss is proportional to surface area, and the heat generation is proportional to the fuel mass flow rate  $\dot{m}_f$  ( $\dot{m}_f = \dot{m}_a \cdot \phi$ ). Thus, the ratio of heat loss to heat generation is proportional to  $L^2/(\dot{m}_a \cdot \phi)$ ; that is, a decline of  $\dot{m}_a$  increases this ratio, making the effects of the heat loss greater, and results in a severe temperature drop near the combustion chamber wall where the flame quenches. This can explain the sharp rise of the lower limit for  $\dot{m}_a$  smaller than 0.037 g/s. On the contrary, as  $\dot{m}_a$  increases, the wider quenching region occurs near the outer wall and restrains the heat generation. This results in the narrower flame stability lower limit. As  $\dot{m}_a$  continues to increase, blow-off in the combustion chamber would be inferred due to the limitations of the chemical reaction time in the flame zone; that is, this is the limitation of the First Damköhler number.

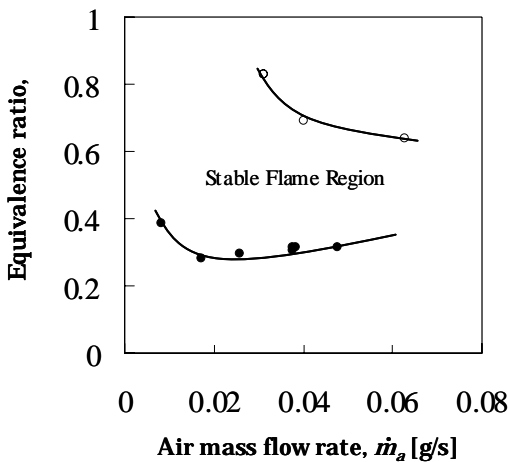


Fig.3 Flame stability limits of ultra-micro combustor

Despite the fact that  $\phi$  was less than 1, there existed an upper limit over a certain  $\dot{m}_a$ . Interestingly, close observation of the phenomenon at the upper limit showed “quenching” rather than “flashback”; that is, with increasing  $\phi$ , the flame separated from the porous surface, and then approached the nozzle surface. Finally, the flame weakened and quenched. The reason for this can be speculated as follows: for combustors, the heat loss flux increases as  $\phi$  becomes larger, and as a result the burning velocity is restrained because the flame temperature decreases. Figure 4 explains the qualitative relationship between the flow velocity of the incoming premixture and the burning velocity versus  $\phi$ . The mean flow velocity  $u$  of the incoming premixture of hydrogen-air passing through the porous late is given by the equation

$$u = \frac{\dot{V}_{H_2} + \dot{V}_a}{S \cdot \sigma}$$

where  $\dot{V}_{H_2}$  is the volume flow rate of hydrogen,  $\dot{V}_a$  is the volume flow rate of air,  $S$  is the porous plate surface,  $\sigma$  is the porosity of the porous plate. From the equations of state for  $\dot{V}_{H_2}$  and  $\dot{V}_a$ , and the relation of the equivalence ratio between  $\dot{m}_{H_2}$  and  $\dot{m}_a$ ,  $\dot{m}_{H_2} = 0.02913 \phi \cdot \dot{m}_a$ ,  $u$  can be expressed as

$$u = \frac{T}{P} \cdot \frac{\dot{m}_a}{S \cdot \sigma} \cdot (0.02913 \cdot \phi \cdot R_{H_2} + R_{air})$$

where  $T$  is the preheated incoming premixture temperature,  $P$  is pressure,  $R_{H_2}$  is the gas constant of hydrogen,  $R_{air}$  is the gas constant of air. At a larger  $\phi$  with heat losses, the flow velocity of the premixture would increase more rapidly than the burning velocity due to the increase of  $T$  by preheating, so that a flame would quench at a certain  $\phi$  over a critical  $\dot{m}_a$ . Further investigation is required into the heat loss effects on the combustion efficiency, because these would have crucial effects on the flame stability of this type of flat-flame combustors.

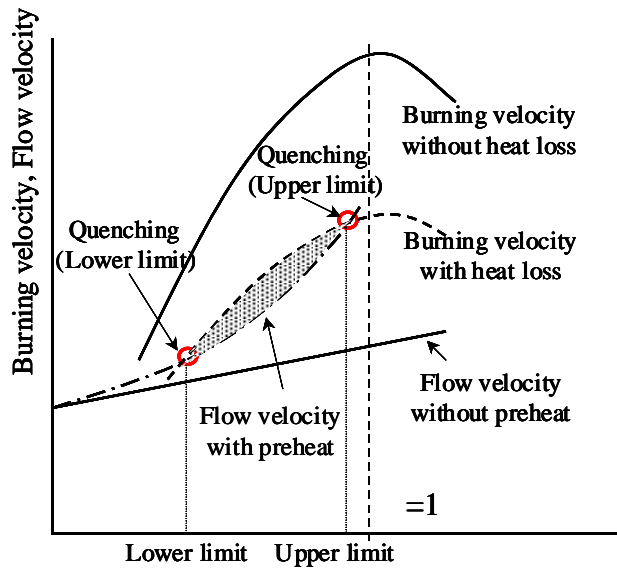
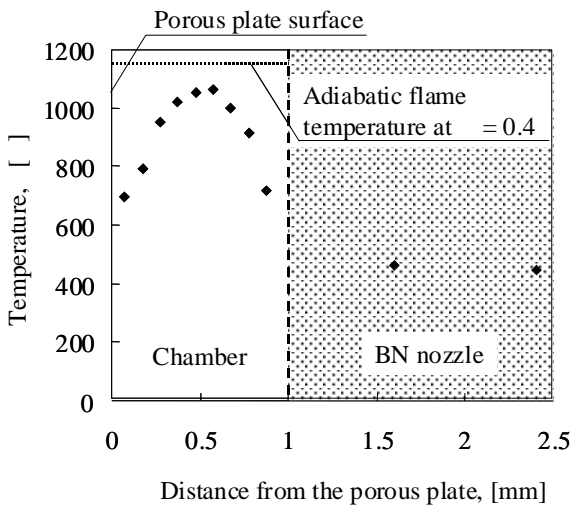


Fig.4 Qualitative explanation for flame stability limits

**Temperature distribution and heat loss**

In order to investigate the combustion behavior in the combustion chamber and the degree of heat loss to the nozzle, temperature distributions were measured preliminary using a sheathed type-K thermocouple [outer diameter: 0.25 mm, thickness of sheath: 50  $\mu$  m, material of sheath: Inconel]. Measurement was performed by inserting the thermocouple into the chamber horizontally via a 1-mm wide vertical slit of the chamber wall, and by moving the thermocouple vertically at a constant radius. In addition, the temperature distributions in the nozzle were measured in 0.8-mm holes drilled radially at fixed heights. The corrections for radiation and conduction losses of the thermocouple were not considered here.

A typical temperature distribution is presented in Fig. 5. After reaching a maximum temperature in the chamber, the temperature declined toward the nozzle surface. The porous plate was found to be heated by heat conduction from the flame. The maximum temperature in the chamber was about 100 K less than the adiabatic flame temperature of hydrogen-air at  $\phi = 0.4$ . This confirmed the occurrence of combustion in the chamber and the existence of considerable heat loss to both the nozzle and to the porous plate. Regarding the heat transfer from the flame, the heat loss to the porous plate was assumed not to have fatal effects on the flame behavior, since the porous plate would exchange sufficient heat with the unburned premixture passing through. However, the heat loss to the nozzle clearly caused a temperature drop. The temperature distributions near the nozzle showed that the heat losses to the nozzle were approximately 20 % of the heat generation of the hydrogen-air premixture of  $\dot{m}_a = 0.037$  g/s at  $\phi = 0.4$ . This assumption was quite close to the heat loss estimation from the temperature distribution in the nozzle. These heat losses would not only worsen the combustion efficiency due to a decrease of the reaction rate, but would also impede the self-sustained operation, if all the losses were conducted to the compressor and turbine.



**Fig.5 Temperature distributions in the chamber and the nozzle at  $\dot{m}_a = 0.037$  g/s and  $\phi = 0.4$**

**Combustion efficiency**

The exhausted gas from the flat-flame combustor was collected at the nozzle slit with a micro-probe (inner diameter: 0.2 mm) made of quartz. The concentrations of unburned hydrogen

were converted into combustion efficiencies. Figure 6(a) shows the combustion efficiency versus  $\phi$  at a constant  $\dot{m}_a = 0.037$  g/s, where the widest flame stable region was obtained. Combustion efficiencies for  $\phi > 0.4$  achieved more than 99.2 %, which confirmed the complete combustion in the chamber. As shown in Fig. 5, the heat loss transferred to the nozzle occurred after the temperature reached the maximum. Despite this heat loss, the hydrogen burned completely. This suggests that the heat loss to the nozzle had little effect on the flat-flame combustion on the porous plate itself, and only caused a temperature decrease of the exhausted gas after complete combustion. For the flame stability upper limits, however, the validity of this consideration has not yet been confirmed, due to the absence of data.

The combustion efficiency decreased drastically for  $\phi < 0.4$ . This suggests that the flame zone became thicker as  $\phi$  decreases and combustion reactions would be inhibited by the heat loss to the nozzle. Finally, the flame quenched due to severe heat losses with which the self-sustained reactions could not maintain. Figure 6(b) shows the combustion efficiency versus  $\dot{m}_a$  at  $\phi = 0.45$ . In this experiment, complete combustion was achieved at a wide range of  $\phi$ , except near the flame stability lower limit.

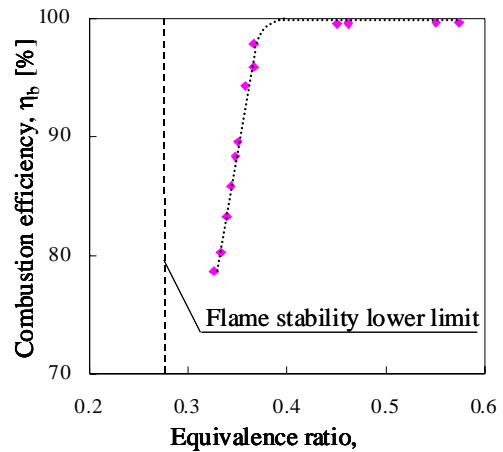


**Fig.6(a) Combustion efficiency versus  $\phi$  at  $\dot{m}_a = 0.037$  g/s**

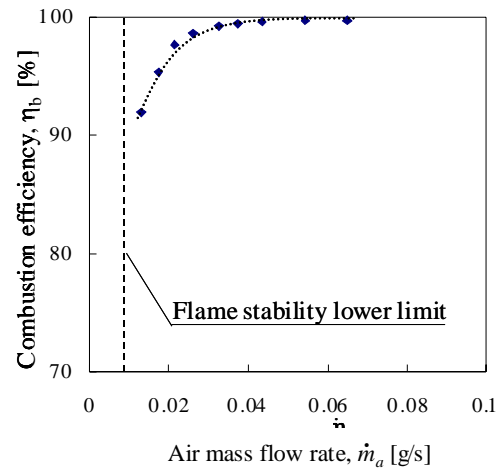


**Fig.6(b) Combustion efficiency versus  $\dot{m}_a$  at  $\phi = 0.45$**

It should be noted that the excellence of the flat-flame burning method using a porous plate in a micro combustor for UMG T was confirmed experimentally. Furthermore, investigation of the combustion mechanism at the upper limit by measuring temperature distributions and combustion efficiencies near this limit must take first priority in future research.

**MICRO COMBUSTOR**

**DESIGN OF A MICRO COMBUSTOR AND EXPERIMENTAL APPARATUS**

**Test sector combustor**

In the research program to make a 3-kW output micro-gas turbine, we will use a turbocharger for passenger cars as the compressor and turbine of the micro-gas turbine. The combustor of the micro-gas turbine should be operated under the conditions of a pressure ratio of 3 and a turbine inlet temperature of 1200 K to match the performance of the turbocharger. A cycle calculation of the micro-gas turbine exerts an air flow rate of 50 g/s, using the assumptions of a combustion efficiency of 99.9%, a turbine efficiency of 75%, and a compressor efficiency of 60%; in addition, an 8% pressure drop in the combustor is needed to achieve high heat release rates. In order to use the available space effectively for making a micro-gas turbine, we produced a rough design of an annular-type hydrogen fueled combustor (inner diameter: 55 mm, outer diameter: 80 mm, length: 30 mm) with 12 fuel injectors as shown in Fig.7. The volume of the combustor was determined in order to obtain a high heat release rate of 200 MW/(m<sup>3</sup>·MPa) at the design point. The power output per one fuel injector of the combustor corresponds to a 100-W class power generator.

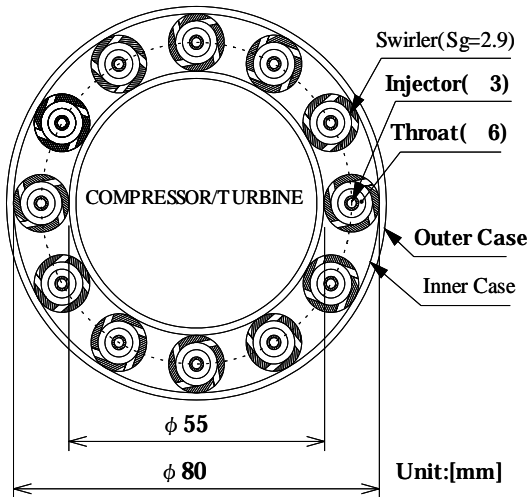


Fig.7 Initial drawing of an annular-type micro combustor

In this study, a 1/4-sector-model test combustor of the annular combustor was prepared to examine its combustion characteristics. Figure 8 shows the sector-model test combustor with 3 fuel injectors and 3 air-inlet swirlers. The test combustor had quartz walls without secondary air holes, and a horizontal combustion-gas exit. Air entered the combustion chamber from swirlers, shown in Fig. 9(a), and air nozzles. The geometrical swirl number of the swirlers was 2.9, and the air-swirling directions of adjoining swirlers were reversed. The throat diameter of the air nozzles was

6.0 mm. Hydrogen was injected through 3 injectors, which were 3.0 mm in diameter. Three types of the injectors with almost the same injection area, shown in Fig. 9(b), were used to examine the effects of the number and direction of the injection holes on the combustion characteristics.

The present experiment was carried out without preheating the air and at atmospheric pressure. Therefore, the air flow rate in this experiment was reduced so as to agree with the air volume flow rate between the present experiment at atmospheric pressure and the practical micro-gas turbine working at 0.3 MPa; 4 g/s (≈ 50 g/s x 1/4 x 1/3). The temperature was measured with a silica-coated R thermo-couple with a 0.1-mm wire diameter. The unburned hydrogen concentration at the exit of the combustor was measured using a quartz tube with a micro orifice and a hotwire-type semi-conductor hydrogen analyzer.

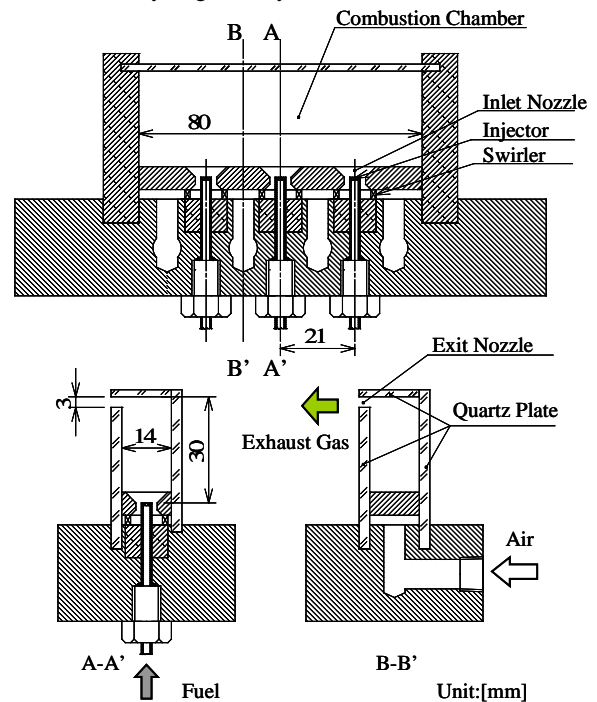
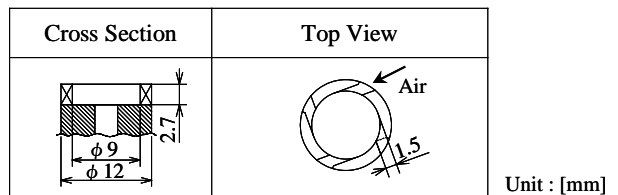


Fig. 8 1/4 sector - model test sector combustor

(a) Swirler



(b) Injectors

Type (Holes area [mm <sup>2</sup> ])	φ 0.4 × 4 (0.50)	φ 0.4 × 4 (0.50)	φ 0.6 × 2 (0.57)
Cross Section	Left Turn	Right Turn	

Fig.9 Swirler (a) and fuel injectors (b)

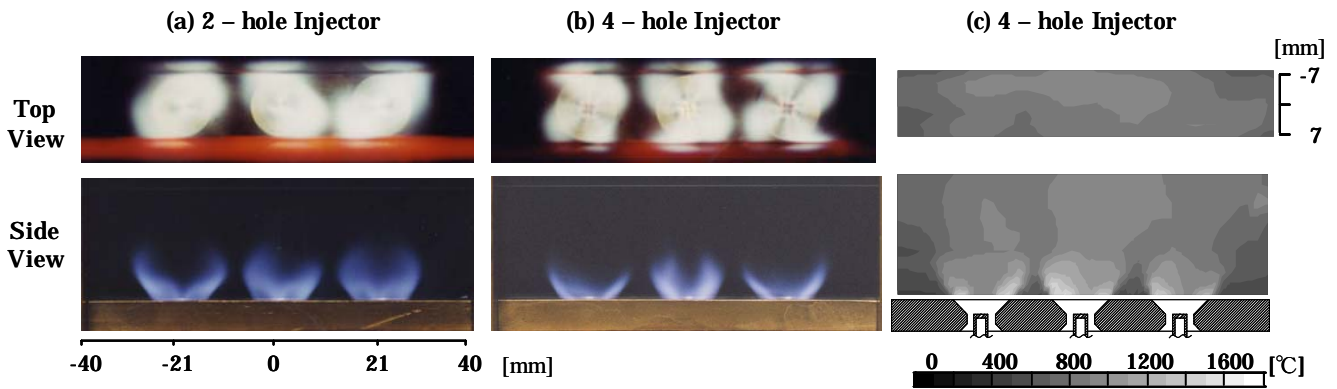


**Fig.11 Hydrogen flame appearances (a,b) and temperature distributions (c) in the test sector combustor at  $\dot{m}_a=4\text{g/s}$  and  $\phi=0.3$**

## EXPERIMENTAL RESULTS AND DISCUSSION

### Flame stability limits

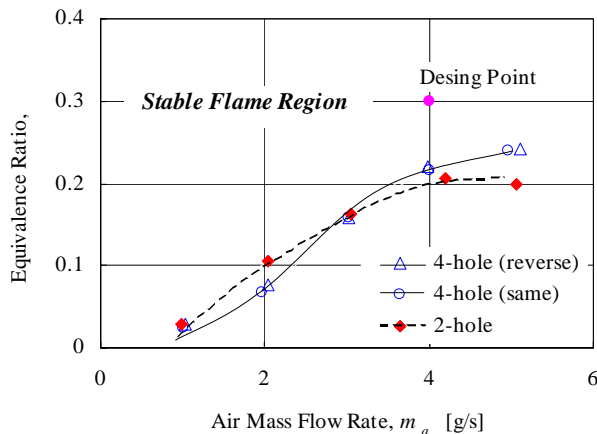


**Fig.10 Stability limits of the test sector combustor**

It was found that three stable flames were easily developed in the combustor at high equivalence ratios. When decreasing the hydrogen flow rate at a fixed air flow rate, the three flames blew off simultaneously at a critical hydrogen flow rate independent of the injector types. Figure 10 shows the flame stability limits of the test sector combustor for the two-hole injector and the four-hole injectors with the same and reverse directions of the swirling air stream. For all the injectors, blow-off limits increase by increasing the air flow rate, and the flame stability region satisfies the design point of the combustor. It can be seen that the stability limit was almost insensitive to the injector types. This suggests that the flame stability of this combustor was preferentially controlled by the air flow field near the injectors due to  $(\rho u)_{\text{air}} \gg (\rho u)_{\text{H}_2}$ .

The flame stability of this combustor was found to be much worse than that of our previous hydrogen combustors with similar structures, configurations and air flow conditions (Yuasa & Goto, 1985, and Yuasa & Goto, 1992), in which the blow-off limits never appeared except during the experiment using a weak swirler with  $S_g=0.45$  (Yuasa & Goto, 1985). The main difference between the present and the previous combustors was the size; the previous ones were about 3 times bigger in dimension and about 10 times larger in

flow rates of hydrogen and air. The observation of the flame bases anchored to the injector rims showed that, for the large combustors, a recirculation zone developing in the swirling air stream expanded upstream beyond the injector exit. For the small combustor, however, the zone expanded only to the injector exits, even for the same air velocities at the air-inlet nozzle throat. This may be attributed to a drastic reduction in the net throat area for the small combustor due to the development of a boundary layer on the nozzle throat wall.

### Flame appearances

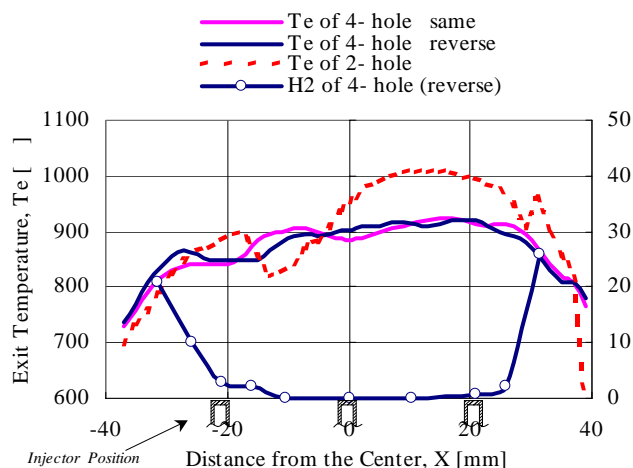
Figure 11(a) shows the flame appearance for the two-hole injectors at the design point. The side view shows that three similar flames develop in the combustor. The flames are installed sufficiently in the combustor, suggesting that the heat release rate of the combustor remained extremely high at the design point. The top view shows that the three flames develop in a zigzag pattern due to the adjoining air streams with reverse swirling motions. The flames have almost the same diameters as the width of the combustor.

Figure 11(b) shows the flame appearance at the design point for the four-hole injectors with injection directions reverse to the swirling coaxial air streams. The lengths of the flames are slightly shorter compared to those of the two-hole injectors, due to the strengthened turbulent mixing with the surrounding air streams by the increasing injection velocities. The top view shows that the four flame pieces corresponding to the injector holes appear in a flame stabilized on the individual injector. The flame pieces are bent in the swirling air stream direction, independent of the hydrogen injection direction. These flame behaviors were similar to the four-hole injectors with the same injection directions to the swirling coaxial air stream. These results suggest that the flow field of the air stream surrounding the hydrogen injector played a crucial role in the determination of the flame behavior, due to the larger momentum of the air streams as a whole.

### Temperature distributions and combustion efficiency

Figure 12 shows the temperature distributions for three types of injectors and the unburned hydrogen concentration for the four-hole injector with reverse hydrogen injection against the air stream. All were measured at the combustor horizontal exit. The

exit temperature distribution of the two-hole injector was not uniform. The highest region coincides with the position where the two flames united as shown in Fig. 11(a). The exit temperature distributions for the two four-hole injectors were seldom different from each other and were more uniform than that of the two-hole injector. The exit temperatures for the four-hole injectors were close to the adiabatic flame temperature of H<sub>2</sub>/Air, 916 °C at  $\phi = 0.3$ . These results show that the four-hole injectors excelled the two-holes injector in the combustion characteristics with respect to flame length and temperature distribution. Figure 11(c) shows the isothermal temperature distributions in the vertical central plane and in the horizontal exit plane. The temperature in the combustor became almost uniform just downstream of the flames. These results for the four-hole injectors suggest that the hydrogen injected into the chamber burned completely. In fact, as shown in Fig. 12, the concentrations of unburned hydrogen at the exit could not be detected except at the region near the side walls where severe heat losses occurred, resulting in a combustion efficiency estimated to be greater than 99.97%.



**Fig.12 Temperature and unburned hydrogen distributions of the test sector combustor at the exit at  $\dot{m}_a = 4\text{g/s}$  and  $\phi = 0.3$**

## CONCLUSIONS

### Ultra-micro combustor

- ☆ To miniaturize gas turbine combustors, shortened diffusion characteristic time and flow laminarization are the most important issues, leading to the concept of a flat-flame burning method.
- ☆ A prototype of a hydrogen-fueled flat-flame ultra-micro combustor with a volume of 0.067 cm<sup>3</sup> for UMGH was developed.
- ☆ Outstanding combustion characteristics related to flame stability, space heating rate, and combustion efficiency were attained, which confirmed that the flat-flame burning method is suitable as a ultra-micro combustor of UMGH.

### Micro combustor

- ☆ A 1/4-sector-model test combustor with three fuel injectors and three air-inlet swirlers was made to examine the combustion characteristics of a hydrogen-fueled annular-type combustor with an air flow rate of 50 g/s for a MGT with a power output of 3 kW.
- ☆ The four-hole fuel injectors and the air swirlers with a strong swirl intensity showed the sufficient performance with respect to flame stability, temperature distribution and combustion efficiency.
- ☆ The flame stability behavior was dependent on whether the recirculation region developing in the swirling air stream expanded upstream beyond the injector exit.

## ACKNOWLEDGMENT

This work was supported in part by the New Energy and Industrial Technology Development Organization (NEDO) of JAPAN for the Proposal-based Energy/Environment International Joint Research Program, "Development of Button-sized Gas Generator Technology," in 2001 and "Leading Research and Development of Ultra Micro Gas Turbines" in 2002. The authors would like to express their thanks to Mr. Sudo, T. for his cooperation in conducting the experiment.

## REFERENCES

- Epstein, A.H., et al., 1997, "Micro-Heat Engines, Gas Turbines, and Rocket Engines —The MIT Microengine Project—," 28<sup>th</sup> AIAA Fluid Dynamics Conference, 4<sup>th</sup> AIAA Shear Flow Control Conference, AIAA 97-1773.
- Fristrom, R.M. and Wstenberg, A., 1965, "Flame Structure", McGraw-Hill, New York.
- Yuasa, S. and Goto, N., 1985, "Combustion Characteristics of Hydrogen in a Test Swirl Combustor for a Micro Gas Turbine", *Transactions of JSME* (in Japanese), Vol.51, No.468, B, pp.2767-2772.
- Yuasa, S. and Goto, N., 1992, "Combustion Performance of a Hydrogen-fueled Small Combustor for a Micro Gas Turbine", *Transactions of JSME* (in Japanese), Vol.58, No.551, B, pp.2288-2295.
- Yuasa, S. and Oshimi, K., 2002, "Concept and Experiment of a Flat-Flame Micro-combustor for Ultra Micro Gas Turbine," 38<sup>th</sup> AIAA/ASME/SAE/ASEE Joint Propulsion Conference, AIAA 2002-3711.